Supporting Information for

Multifunctional binder $3M_x$ for improving the cycle stability of rechargeable Li-S batteries

YuRui Wu†, Ming Yang†, YaQun Zou, SiYao Hou, BoWen Hu, ShuiMiao Wang, Yong Tao*, ChangAn Yang*

College of Chemistry and Chemical Engineering, Hunan Institute of Science and Technology, Yueyang 414006, Hunan Province, PR China.

E-mail: Chang_anyang@hnist.edu.cn, ivy_tao0630@hotmail.com

Material Characterization.

The NMR measurement was performed on an AV400 MHz spectrometer from Bruker, using $CDCl_3$-d6 as the solvent and tetramethylsilane (TMS) as the internal standard at ambient temperature. The structure of the material is analyzed by Fourier Transform Infrared Spectrometer (FT-IR, Vector-22, Switzerland) in the range of 400-4000 cm^{-1}. The morphology of the electrodes before and after the cycle was observed and analyzed by the Zeiss Sigma300 field emission scanning electron microscope. The high vacuum mode was adopted at room temperature, and the accelerating voltage was 5-15 kV. The chemical composition of the electrode surface is analyzed by EDS. The batteries are disassembled in a glove box filled with argon gas, and the electrodes are thoroughly cleaned with electrolyte, the electrolyte is 1M LiTFSI dissolved in a volume ratio of 1:1 1,3-dioxolane (DOL)/ethylene glycol dimethyl ether (DME) mixed with 2% $LiNO_3$. The concentration of lithium polysulfide in the solution was measured by UV-Vis spectrophotometer (UV-Vis) in the range of 600-300 nm to compare the adsorption capacity of different binders for polysulfide. The concentration of lithium polysulfide solution is 5 $mg \cdot mL^{-1}$, and the time interval between each UV-Vis measurement was 2 hours.

Supplemental Figures.

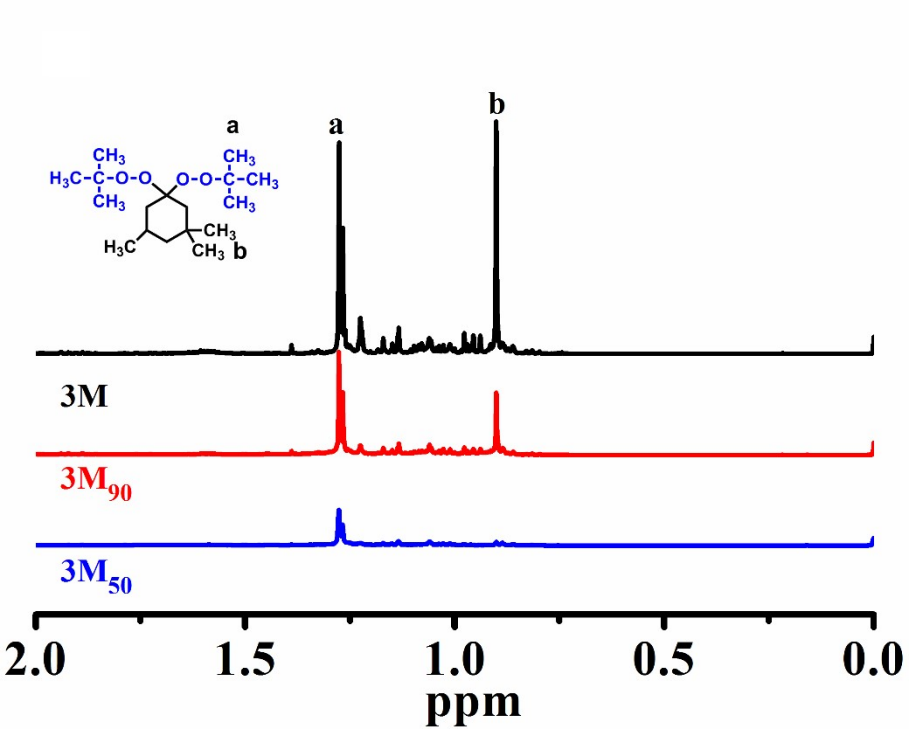

Figure. S1 [1]HNMR comparison of 3M,$3M_{90}$ and $3M_{50}$

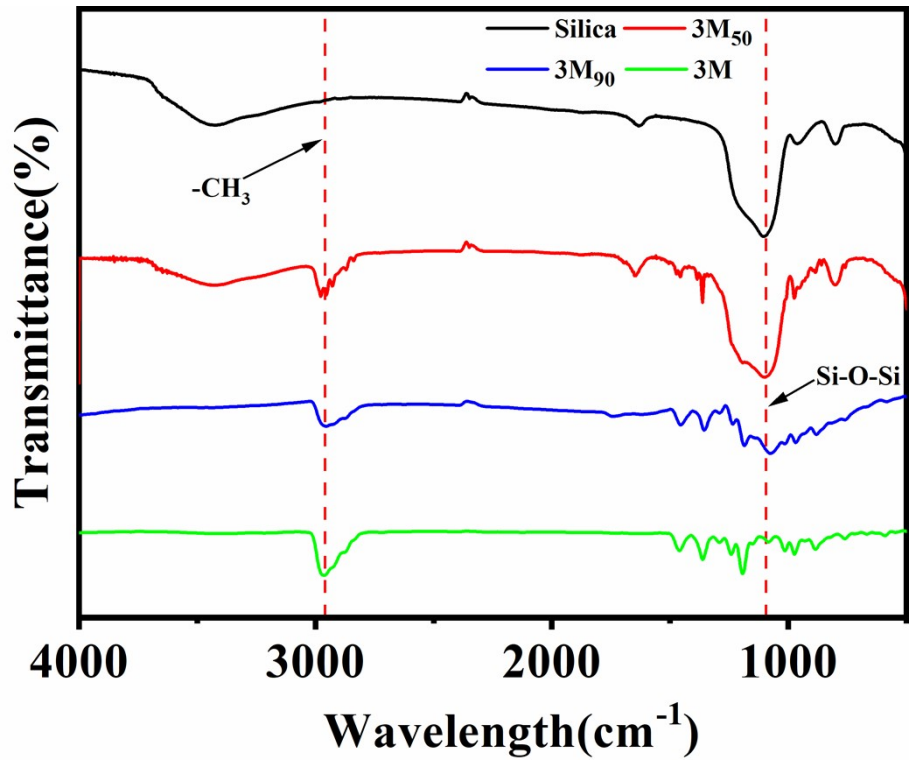

Figure. S2 FT-IR spectra of Silica,$3M_{50}$,$3M_{90}$ and 3M

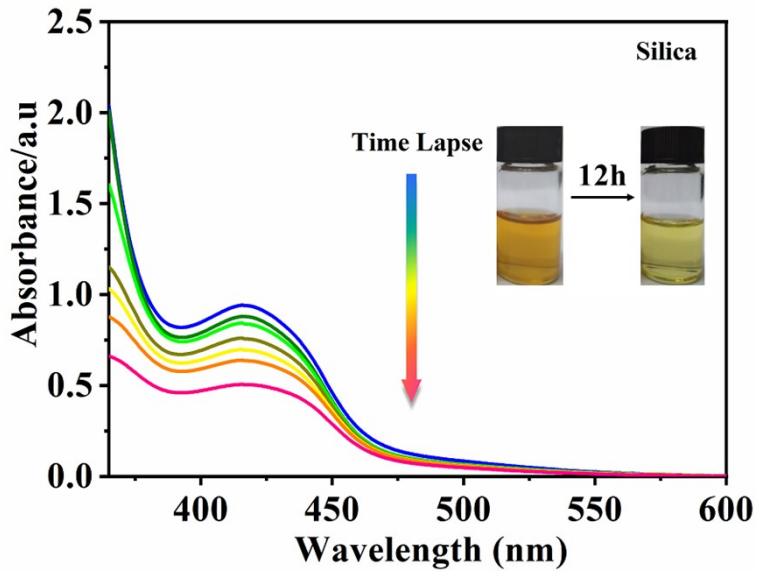

Figure. S3 UV-Vis absorption spectra and optical images of the polysulfide (average formula Li_2S_6) solution with silica binder

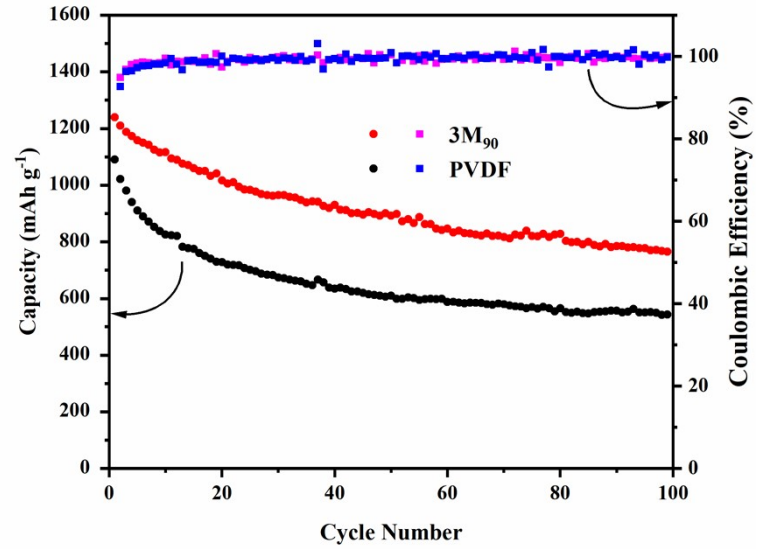

Figure. S4 Cycling performance of Li-S batteries with $3M_{90}$ and PVDF binder at 0.1C

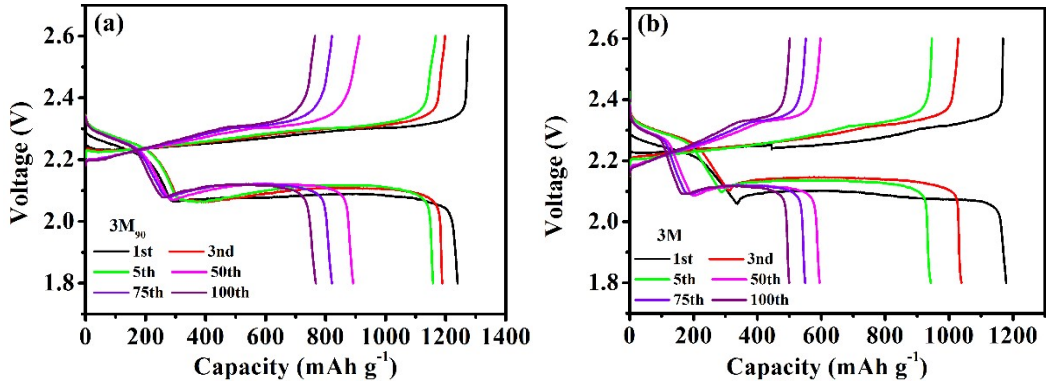

Figure. S5 Discharge/charge profiles of Li-S batteries in different cycles at 0.1C

based on **(a)** $3M_{90}$ binder and **(b)** 3M binder

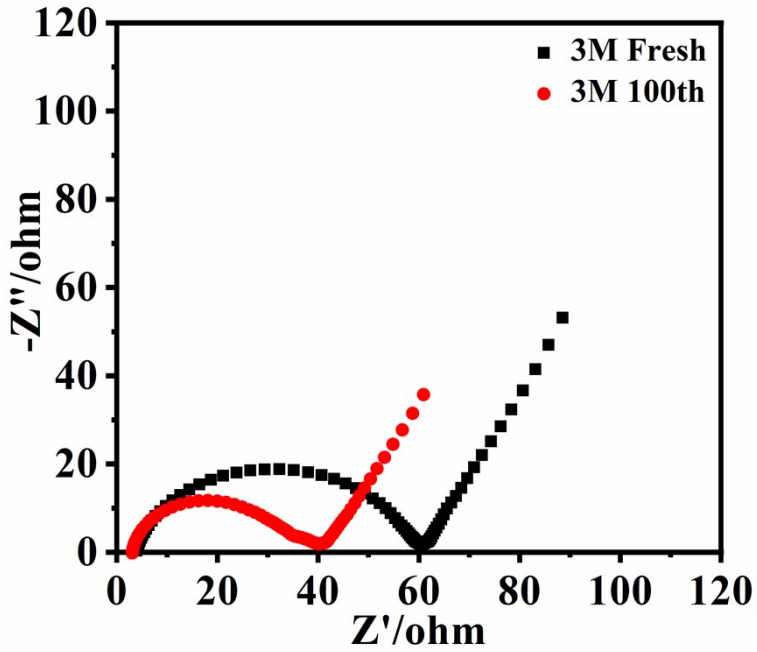

Figure. S6 EIS data of the Li-S batteries with 3M binder before and after the 100th cycle at 0.1 C

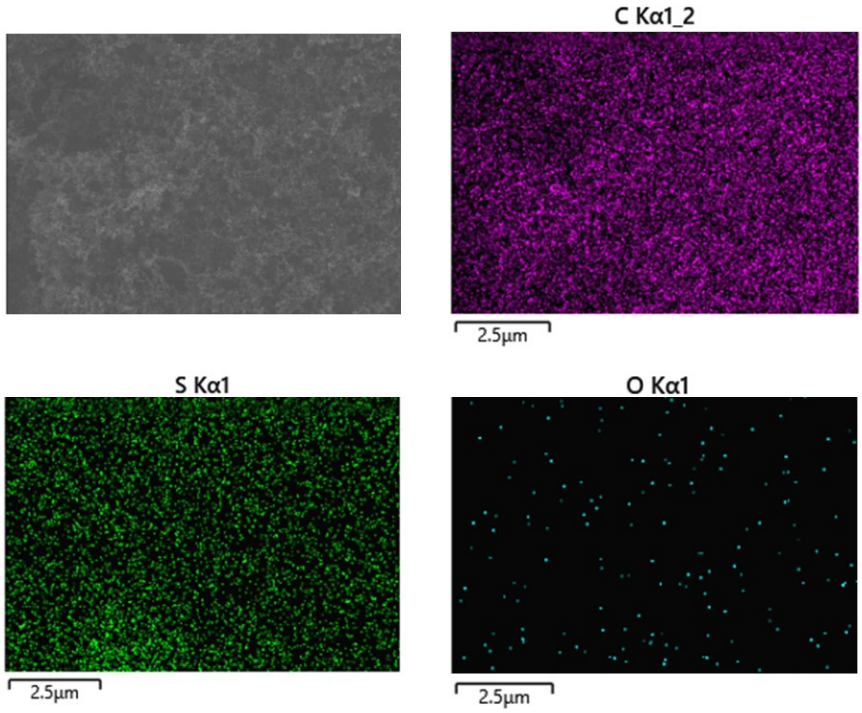

Figure. S7 Energy dispersive X-ray spectroscopies of the pristine electrode containing 3M binder.

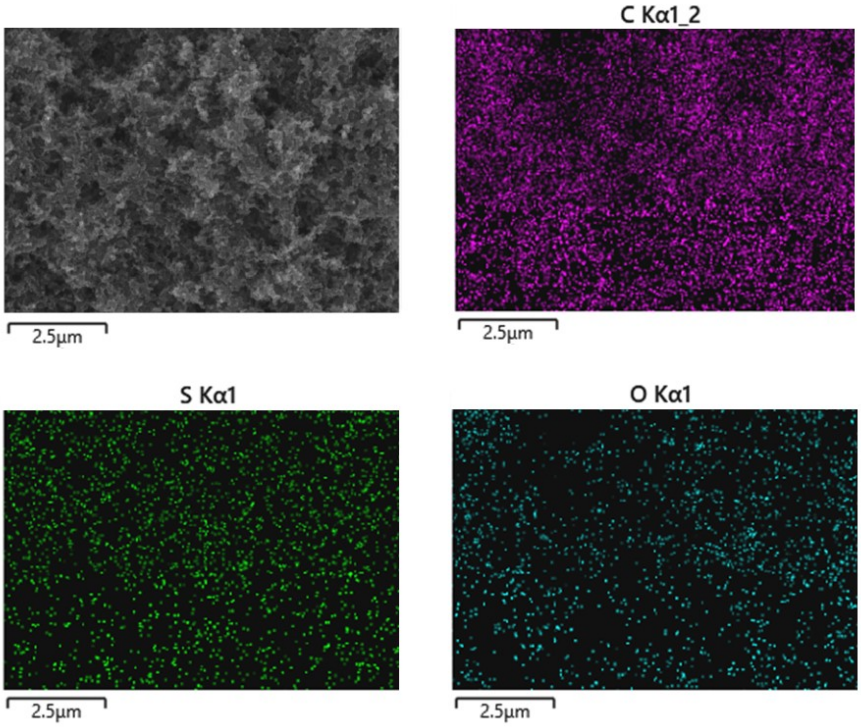

Figure. S8 Energy dispersive X-ray spectroscopies of the fully charged electrode containing 3M binder.

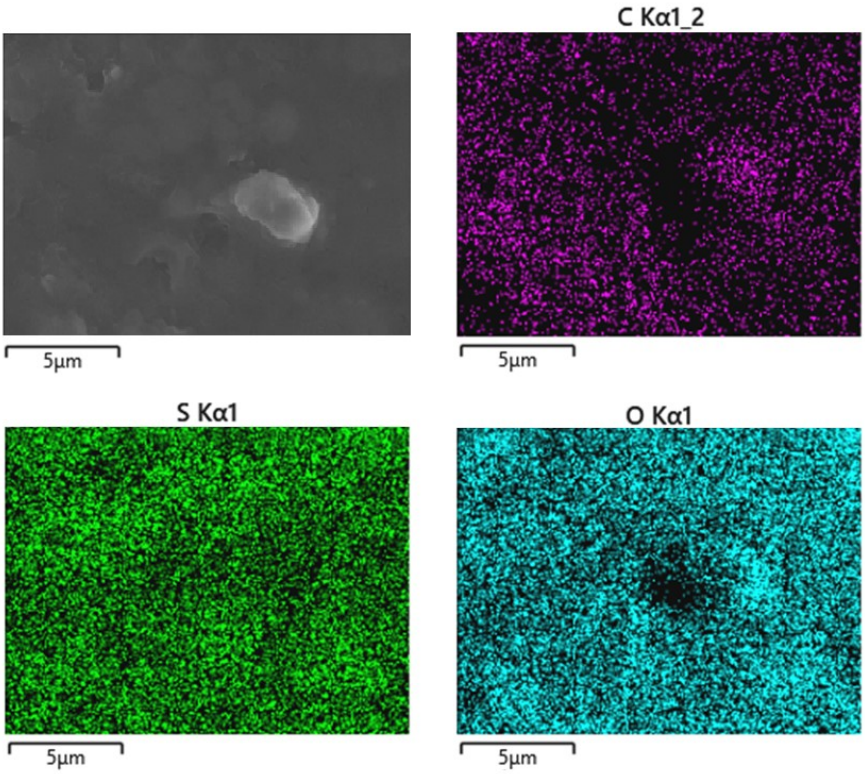

Figure. S9 Energy dispersive X-ray spectroscopies of the fully discharged electrode containing 3M binder.

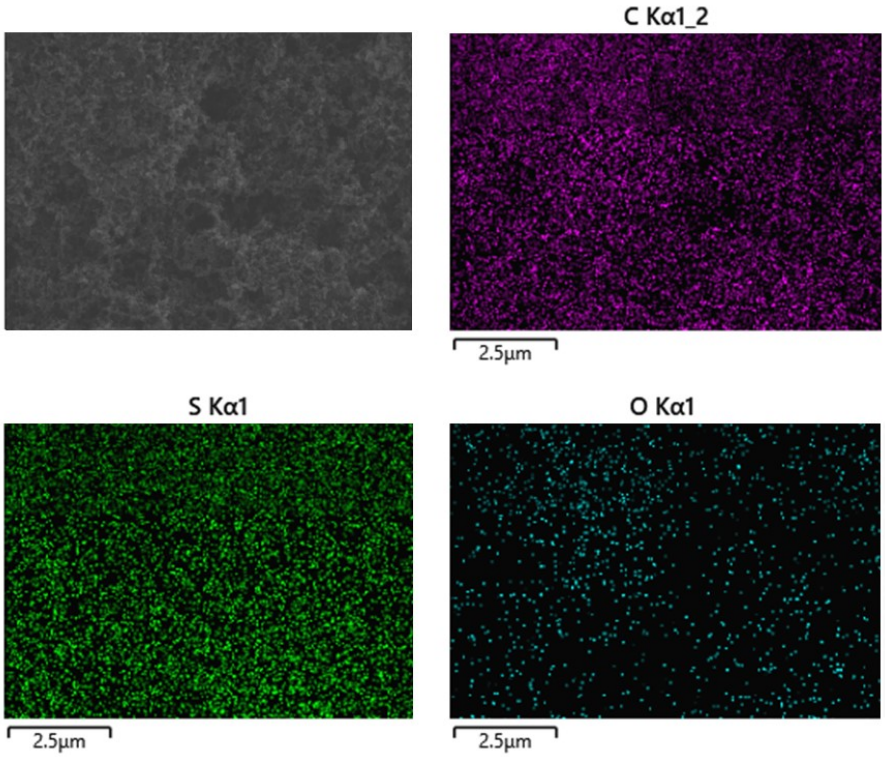

Figure. S10 Energy dispersive X-ray spectroscopies of the pristine electrode containing Silica binder.

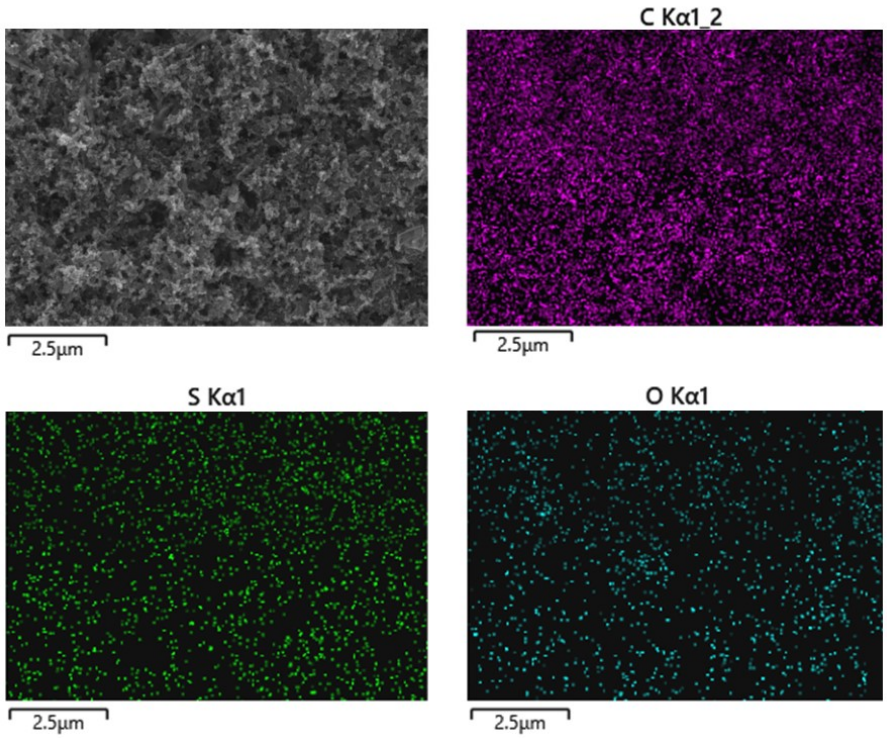

Figure. S11 Energy dispersive X-ray spectroscopies of the fully charged electrode containing Silica binder.

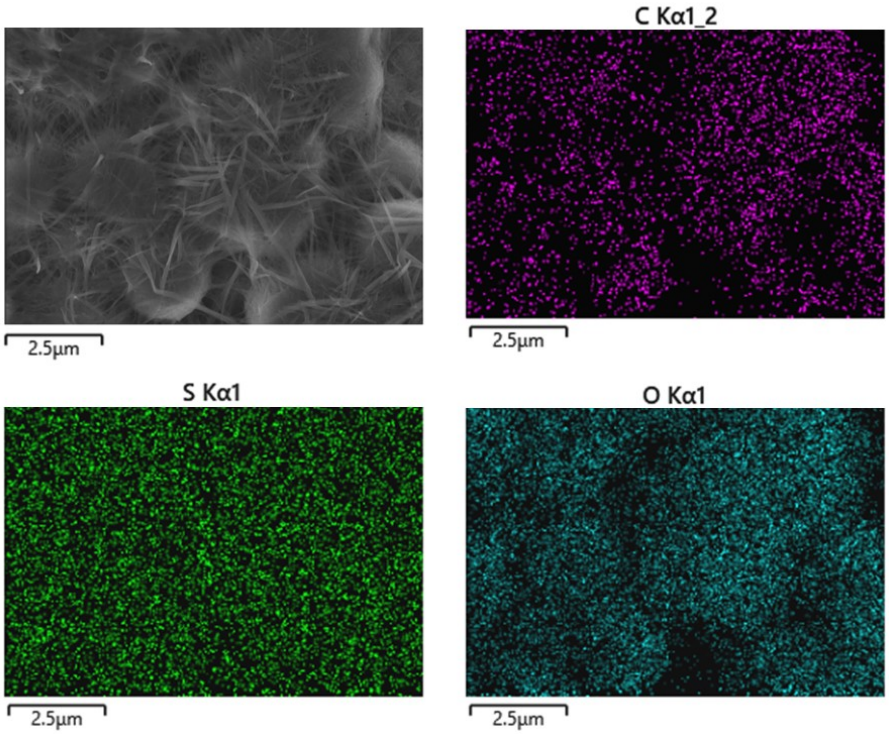

Figure. S12 Energy dispersive X-ray spectroscopies of the fully discharged electrode containing Silica binder.

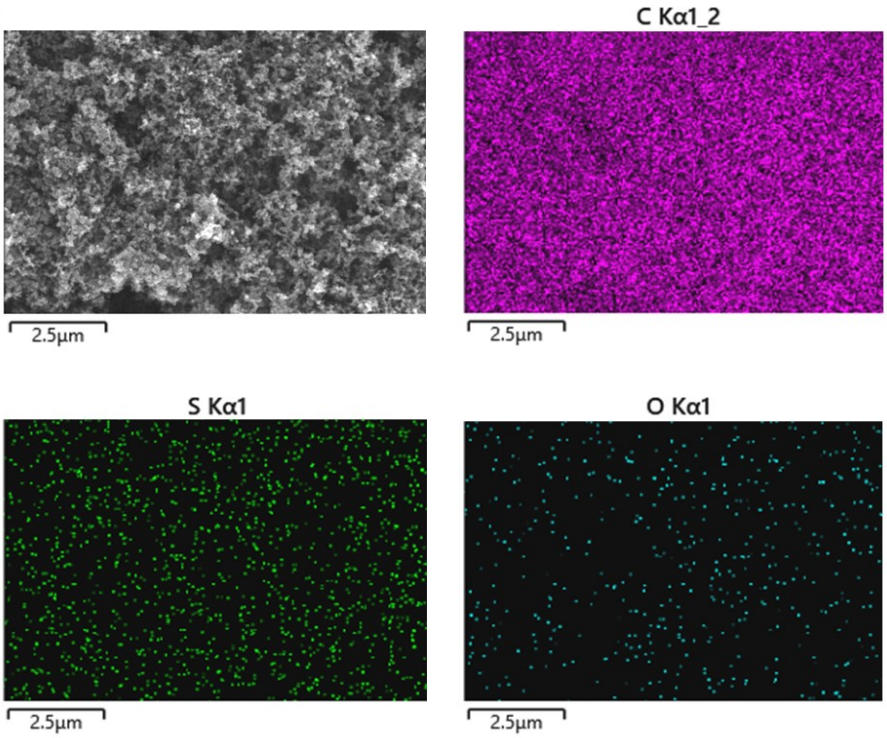

Figure. S13 Energy dispersive X-ray spectroscopies of the pristine electrode containing $3M_{90}$ binder.

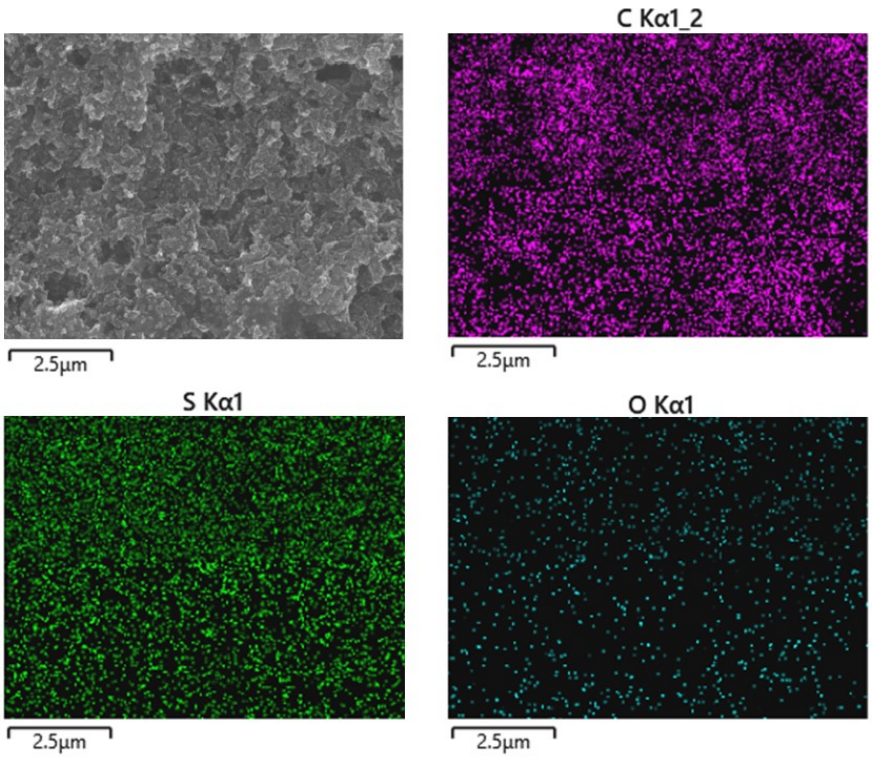

Figure. S14 Energy dispersive X-ray spectroscopies of the fully charged electrode containing $3M_{90}$ binder.

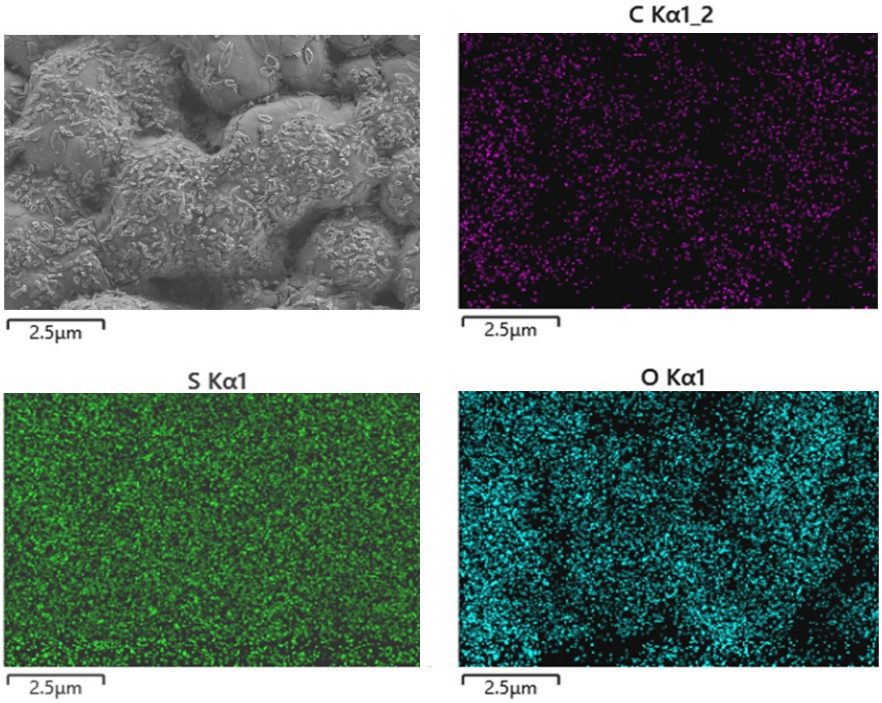

Figure. S15 Energy dispersive X-ray spectroscopies of the fully discharged electrode containing $3M_{90}$ binder.